# Characterization of Cyanine Dye-Labeled Poly(*N*-isopropylacrylamide) Core/Shell Microgels Using Fluorescence Resonance Energy Transfer

**Clinton D. Jones, Jonathan G. McGrath, and L. Andrew Lyon***

*School of Chemistry and Biochemistry, Georgia Institute of Technology, Atlanta, Georgia 30332-0400*

*Received: July 25, 2003; In Final Form: May 26, 2004*

The swelling behavior of the core component in poly(*N*-isopropylacrylamide) (pNIPAm) core/shell microgels is investigated via fluorescence resonance energy transfer (FRET). Photon correlation spectroscopy (PCS) data show that the cross-linked polymer network in the core is hindered from expanding to its maximum volume in the presence of the added shell. Covalent attachment of the sulfoindocyanine donor/acceptor pair of Cy5/Cy5.5 to the core component allows investigation of the core swelling behavior with FRET. In the absence of the shell, only a small degree of energy transfer is observed in the core when it is swollen to its maximum volume below the pNIPAm lower critical solution temperature (LCST) of 31 °C. Addition of a pNIPAm shell produces a significant degree of FRET under the same solution conditions, illustrating that the polymer chains in the core adopt a constrained conformation relative to their fully swollen state. The volume phase transition behavior of the fluorescently labeled core and core/shell particles was interrogated with PCS and correlates well with FRET analysis over the same temperature range, providing evidence that donor and acceptor molecules are homogeneously distributed throughout the core. The structure−function relationship between the core and shell is explained in terms of a radially distributed cross-linker density gradient created in the core and shell components during the two-stage particle synthesis. Furthermore, these analyses allow for calculation of the actual shell thickness, as the apparent shell thickness obtained from PCS measurements underestimates the actual thickness by an amount equivalent to the compression-induced core radius decrease.

## Introduction

Investigation of fundamental structural relationships on the nanoscale often requires science to move beyond the conventional analytical techniques of a particular field. In the case of polymer colloids, light scattering and electron microscopy provide information concerning particle size and distribution,[1] while revealing architectural[2] and topological details.[3] Both techniques report on the outermost portion of the particle and its immediate surroundings, with a few exceptions.[4,5] The characterization of multilayered nanoparticles becomes complicated due to the need to characterize the inner portion of the particle. In this investigation, we use the technique of fluorescence resonance energy transfer (FRET) to probe the swelling behavior of hydrogel polymer chains inside the core component of core/shell hydrogel nanoparticles. FRET is a distance-dependent process requiring that two fluorophores, termed the donor and the acceptor, have overlapping emission and excitation spectra, respectively.[6] Energy transfer occurs from excited donor molecules to acceptor molecules when the two are within a certain distance of each other. The intrinsic distance of the particular fluorophore pair at which FRET is 50% efficient is referred to as the Förster radius ($R_o$). Energy transfer is the result of long-range dipole-induced dipole interactions.[6] In this work, the long-wavelength excitable sulfoindocyanine-based dyes Cy5 and Cy5.5 (Amersham Biosciences) were chosen as the donor and acceptor molecules, respectively. This fluorescent pair has been shown to have a large $R_o$ value of 68.7 Å in aqueous media.[7]

Our group has focused on the synthesis and characterization of polymer nanoparticles having a core/shell type morphology, where environmentally responsive polymers comprise both the core and shell components.[2,8−11] Such hydrogel nanoparticles (microgels) are cross-linked, spherical, colloidal particles ranging in diameter from 10 to 1000 nm and are individually composed of a network of randomly oriented polymer chains that have the ability to exist in a swollen or collapsed state depending on local environmental conditions.[12−15] Microgels composed of the environmentally responsive polymer poly(*N*-isopropylacrylamide) (pNIPAm) undergo a temperature-induced, reversible phase transition at 31 °C as a result of the lower critical solution temperature (LCST) of the polymer.[16,17] We have prepared core/shell microgels for fundamental studies by designing particles with multiple volume phase transitions[2] along with investigating the dynamics and mechanisms of particle phase transition behavior.[10,18] The core/shell structure can be elucidated via photon correlation spectroscopy (PCS) by monitoring size differences between the core and core/shell particles.[2,8] Our core/shell particles typically are not highly interpenetrated and do possess two distinct components as illustrated with electron microscopy.[2] Previous fluorescence investigations have also indicated that the interface between the core and shell components lacks a large degree of network interpenetration.[10]

Recent investigations involving pNIPAm-*co*-acrylic acid (core)/pNIPAm (shell) microgels illustrate that the swelling ability of the core is indeed modulated by the shell.[8,11] The pH-responsive nature of the core in this case allowed isothermal investigations of particle size changes by variation of solution conditions. Increasing the solution pH to above the acid p$K_a$ (4.25)[19] results in a particle volume increase due to Coulombic

* To whom correspondence should be addressed: lyon@chemistry.gatech.edu.

10.1021/jp0361834 CCC: $27.50 
Published on Web 07/29/2004

**CHART 1: Molecular Structures of the NHS-Functionalized Cyanine Dyes**

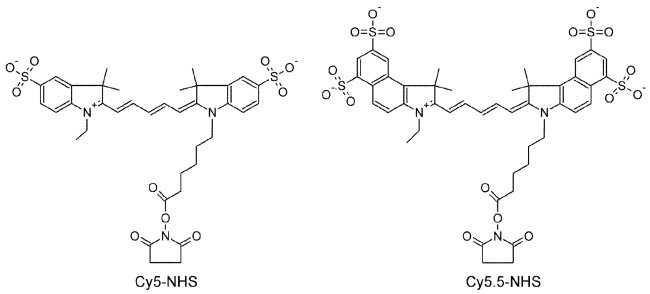


repulsion between charged groups and added osmotic pressure (Donnon effect) from incorporated counterions.[20,21] PCS data show that the pNIPAm shell restricts the core from swelling to its native volume both above and below the p$K_a$ of acrylic acid at temperatures below 31 °C. When compared to the volume of the parent core particle at a pH above the p$K_a$, the core/shell structure actually displays a *smaller* volume due to this compression effect.[8,11] Also under these pH conditions, the parent core particle undergoes only small temperature-induced volume changes above 31 °C due to the extreme amount of Coulombic repulsion in the network. However, the addition of a pNIPAm shell results in compression of the core and induces a large volume change above the pNIPAm LCST, evidently overcoming the charge repulsion in the core to deswell the particle. The current investigation involves a pNIPAm core containing a small percentage of amine groups for post-polymerization modification with *N*-hydroxysuccinimidyl (NHS) ester-functionalized cyanine dyes, shown in Chart 1. The shell is composed of pNIPAm, and both the core and shell components are lightly cross-linked with *N*,*N*′-methylene(bisacrylamide) (BIS). The amount of energy transfer occurring between the cyanine donor/acceptor pair in the core component is monitored by comparing the emission intensity of the donor and acceptor molecules in the absence and presence of the shell over a range of temperature values. These studies provide two main findings. First, they confirm our previous indirect measurements of core compression using the more direct method of FRET, and second, they allow for accurate calculation of the actual shell thickness. PCS studies alone are insufficient for shell thickness calculations, as the apparent particle size increase is a convolution of the shell thickness and the core compression. By independently measuring the core compression using FRET, the thickness of the hydrogel shell added under specific synthetic conditions can be directly determined.

## Experimental Section

**Materials.** All reagents were purchased from Sigma-Aldrich unless noted otherwise. *N*-Isopropylacrylamide (NIPAm) was recrystallized from hexanes (J. T. Baker) and dried in vacuo prior to use. *N*,*N*′-Methylene(bisacrylamide) (BIS), sodium dodecyl sulfate (SDS), and ammonium persulfate (APS) were used as received. *N*-(3-Aminopropyl)methacrylamide hydrochloride (APMA) was purchased from Polysciences and used as received. Monofunctional *N*-hydroxysuccinimidyl (NHS) esters of Cy5 and Cy5.5 were purchased from Amersham Biosciences and used as received. Water for all reactions, solution preparation, and polymer purification was first distilled then deionized to a resistance of 18 MΩ (Barnstead E-Pure system) and finally filtered through a 0.2-$\mu$m filter to remove particulate matter.

**Core/Shell Microgel Synthesis.** Core/shell microgels were synthesized via two-stage free-radical precipitation polymerization as previously reported.[8] Core particles were first synthesized by dissolving NIPAm (5.00 mmol), BIS (0.2627 mmol; yields 5% cross-linked particles), APMA (0.0106 mmol), and SDS (0.083 mmol) into 75 mL of $H_2O$ and heating to 70 °C under nitrogen. Free-radical polymerization was initiated with a 0.5 mL of APS (0.123 mmol) solution and allowed to proceed for 5 h at 70 °C under nitrogen. Shell addition was performed by using core particles as nuclei in the subsequent precipitation polymerization of a feed of differing monomer composition.[2,8] First, a 5.0 mL portion of the core particle solution together with SDS (0.002 mmol) was added to 15.0 mL of water and heated to 70 °C under nitrogen. Although core particle solutions contain SDS, added surfactant is necessary for stabilization during heating and subsequent shell polymerization. After thermal equilibration of the core solution, 5 mL of an aqueous monomer solution containing NIPAm (0.4745 mmol) and BIS (0.0097 mmol; yields 2% cross-linked shells) was heated separately to 70 °C under nitrogen and then added to the core solution under monomer-flooded conditions. Free radical polymerization was then initiated with 0.5 mL of an APS (0.004 mmol) solution, and polymerization was allowed to proceed at 70 °C under nitrogen for 5 h. All particles used for analysis were purified via dialysis (Spectra/Por 7 dialysis membrane, MWCO 10 000, VWR) against daily changes of $H_2O$ for 2 weeks at 5 °C.

**Fluorescent Labeling.** The dyes used in these studies are not tolerant to free-radical polymerization conditions. Thus, a routine scheme for postpolymerization modification of the microgels is employed. Furthermore, it should be noted that core/shell particles are labeled following shell addition instead of adding shells to prelabeled core particles. Stock solutions of Cy5 and Cy5.5 were prepared by dissolving 1 mg of each NHS-ester functionalized dye separately into 5.0 mL of anhydrous dimethylformamide and stored under nitrogen. Amide bond formation between the amine moieties in the microgels and the NHS-ester-functionalized dyes was performed at room temperature in pH 7.0, 0.01 M $NaH_2PO_4$ buffer overnight. Particles containing only one fluorescent dye were prepared by dispersing 0.2 mL of the purified microgel solution into 0.8 mL of phosphate buffer. An equimolar amount ($NH_2$:Cy dye) of the corresponding fluorophore stock was then added to the buffered mixture. Particles containing both Cy5 (donor) and Cy5.5 (acceptor) molecules were prepared in the same manner with only half the molar equivalent of each dye added in this case. The fluorescently labeled particles were purified by centrifugation (16 100*g*, 70 min) at 25 °C, followed by removal of the supernatant solution and redispersion of the particles in $H_2O$ five times.

**Characterization.** Microgel sizes and polydispersities were determined via photon correlation spectroscopy (Protein Solutions Inc.) as previously reported.[8] Samples were analyzed in a three-sided quartz cuvette into which was placed 0.5 mL of a 10 $\mu$g/mL particle solution. The sample was allowed to equilibrate at the proper temperature for 5 min before data collection. Longer equilibration times did not lead to variation in the measured particle size, scattering intensity, or polydispersity. Scattered light was collected at 90° by a single-mode optical fiber coupled to an avalanche photodiode detector. Data were analyzed with Protein Solutions' Dynamics Software Version 5.25.44. Each data point reported here is an average of five separate size determinations. Each size determination consists of 25 total measurements, which individually have a

5 s integration time. Note that the algorithms used for determination of the translational diffusion coefficient allow for non-Gaussian and/or multimodal populations. In all cases, only one particle population is observed with the relative polydispersity of the population being less than ±15%.

Fluorescence analysis was performed on a temperature controlled steady-state fluorescence spectrophotometer (Photon Technology International), equipped with a Model 814 PMT photon-counting detector. Measurements were performed in a quartz cuvette, and the stirring sample solution was allowed to equilibrate at the proper temperature for 5 min prior to data collection. The cell temperature was controlled with a PE 60 Temperature Controller & Peltier Stage (Linkam Scientific Instruments Ltd., Surrey, UK). The slits were adjusted to achieve a bandwidth of 3.0 nm, and the spectra were measured with a step size of 1 nm and a 1 s integration time. The excitation wavelengths used for Cy5 and Cy5.5 were 646 and 674 nm, respectively. Fluorescence resonance energy transfer FRET measurements of microgel solutions were made at a particle concentration of ~10 $\mu$g/mL at an excitation wavelength of 646 nm. Emission intensity ratios were measured at 671 nm ($I_D$) to that at 697 nm ($I_A$) corresponding to the Cy5 donor and Cy5.5 acceptor emission energies, respectively.

## Results and Discussion

Cross-linked pNIPAm microgels undergo a temperature induced volume change at ~31 °C, which is the intrinsic LCST of the parent polymer.[12,14,17] In the hydrophilic swollen state, water swells the microgels, where hydrogen bonding occurs between water and amide groups along individual polymer chains. Hydrogen bonding is disrupted as the local solution temperature is increased from below to above the polymer LCST. This entropically favored expulsion of water from the polymer matrix, along with hydrophobic and hydrogen bonding interactions between neighboring polymer chains, induce the particles to undergo a large-magnitude volume change as a function of temperature. The detailed volume phase transition (VPT) behavior of microgels can largely be attributed to the particle preparation method, precipitation polymerization. Particle formation occurs in aqueous solution upon temperature-induced free-radical initiation with ammonium persulfate at 70 °C. At this temperature, water-soluble monomers polymerize to form oligomer chains that are insoluble upon reaching a certain critical chain length due to the LCST of pNIPAm. These chains undergo hydrophobically favorable coil-to-globule phase transitions and aggregate with other globules to form precursor particles, which then aggregate and grow to form colloidally stable microgels. Stabilization occurs due to both surfactant adsorption and charge incorporated on the growing particles from the initiator fragments.[12,14] During particle growth, *N,N′*-methylene(bisacrylamide) (BIS) cross-linker is statistically incorporated faster than other constituent monomers leading to the creation of a radial distribution of cross-links.[10,13,22,23] Considering this process, the core component possesses a greater polymer network density toward the interior and more loosely cross-linked chains toward the periphery. Chains close to the particle periphery have more degrees of freedom and are able to extend over longer length scales in a good solvent. The gradient model is sufficient for describing the internal microgel structure for cross-linker concentrations below 7 mol % as experimentally shown by others.[24,25]

Because the synthetic conditions are the same for shell addition, a radial cross-linking density gradient is expected in the shell component as well for loosely cross-linked systems, with the greatest polymer network density being located at the interface of the core and shell.[8] In the second stage of the core/shell synthesis, collapsed core particles serve as preexisting hydrophobic nuclei and capture growing oligomers from solution to form the shell component. Upon particle reswelling below 31 °C, the rigid interior (more highly cross-linked portion) of the shell component prohibits the core from expanding to its maximum volume before shell addition. Therefore, the same population of loosely cross-linked chains near the core periphery are hindered from reaching their fully extended state in the presence of added material (e.g. the shell).[8] If heterogeneity were not present within both the core and shell in the form of a radial cross-linking density gradient, one would not expect to observe such effects, as the core and shell would have *the same average and local* cross-linker concentration. The average number of chains that are perturbed will differ according to the cross-linker concentration, with lower mol % cross-linked particles having a higher average number of loosely cross-linked chains near the periphery than highly cross-linked particles (above 7 mol % BIS) that do not have a well-defined gradient morphology.[25] The system presented here is a specialized one in that the core (5% BIS) possesses a higher average cross-link density than the shell (2% BIS). This design is advantageous for these studies, in that *any* observation of core compression can only be attributed to a cross-link gradient, since a more loosely cross-linked shell cannot induce compression in the absence of heterogeneous cross-link incorporation.

While this dendritic morphology is fundamentally interesting with respect to the particle swelling properties, it presents a real difficulty in accurately determining the amount of polymer added in the second polymerization stage. Knowing the shell thickness with some degree of accuracy is an extremely important aspect of this work. For hard material core/shell particles such as metal and semiconductor core/shell nanoparticles, high-resolution TEM is a standard method for quantifying the amount of added material. This technique is insufficient for detailed analysis of soft, solvent swollen materials such as hydrogel nanoparticles that dehydrate under vacuum and deform upon immobilization on a surface. Naively, one could expect routine PCS analysis would offer a measure of shell thickness using the equation,

$$(R_{\text{shell}})_T = (R_{\text{h,core/shell}})_T - (R_{\text{h,core}})_T \quad (1)$$

where $(R_{\text{shell}})_T$ is the shell thickness, $(R_{\text{h,core/shell}})_T$ is the average hydrodynamic radius of the core/shell particle, and $(R_{\text{h,core}})_T$ is the average hydrodynamic radius of the parent core particle. The *T* subscript indicates radius values at a specific temperature, as the measurement is a temperature-dependent one. Given our previous studies of core compression, it is clear that eq 1 is incorrect. Instead, a more appropriate measure of shell thickness is obtained from:

$$(R_{\text{shell}})_T = (R_{\text{h,core/shell}})_T - (R_{\text{h,core}})_T + (\Delta R_{\text{h,core}})_T \quad (2)$$

where $(\Delta R_{\text{h,core}})_T$ is the *decrease* in average hydrodynamic radius of the core due to compression. This last term is invisible to the PCS measurement and thus must be determined by an independent method. As described above, the method chosen here is FRET, which will report the mean change in donor−acceptor distance in the core, and thus the change in core volume due to compression.

The core/shell system chosen for this investigation is analogous to pNIPAm homopolymer microgels; the core and shell components are both composed of the same material. A small

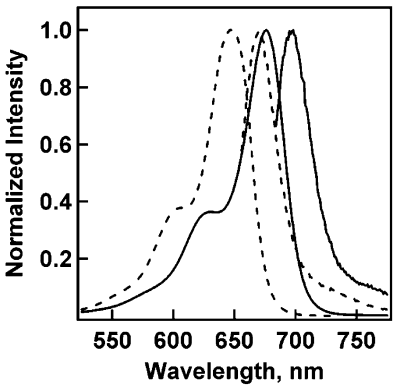


**Figure 1.** Absorbance and emission spectra of core particles containing only donor (Cy5) or acceptor (Cy5.5) dye molecules. The dashed line represents absorbance and emission from Cy5 labeled microgels showing values of 646 and 671 nm, respectively. The solid line represents the Cy5.5 labeled microgels showing absorbance and emission at 674 and 697 nm, respectively. Absorbance spectra were collected with a UV−vis spectrophotometer. Emission spectra were collected upon excitation of the Cy5 donor and Cy5.5 acceptor at 646 and 674 nm, respectively.

amount of amine containing comonomer (0.2 mol %) was incorporated into the core for the sole purpose of modifying the particles with NHS-ester-modified cyanine dyes in a postpolymerization step. The donor/acceptor pair Cy5 and Cy5.5 was chosen due to the ease of incorporation into aqueous-based systems, their large quantum efficiencies, and the large Förster radius (∼68.7 Å) for the pair.[7] The low photon energies needed to excite the dyes also reduces the scattering cross-section of the polymer particles in solution during fluorescence analysis. To our knowledge, this is the first use of cyanine-based dyes as probes for synthetic hydrogels. The monofunctional NHS ester of both Cy5 and Cy5.5 was used to covalently attach the dyes inside of the anime-functionalized core. The amine groups react with the ester to form an amide bond between the dyes and the polymer chains.[26] Figure 1 shows the spectral properties after incorporating each individual dye separately into the core microgels used in this study. The excitation and emission wavelengths of the cyanine dyes are not perturbed in either case and are the same for each dye before and after incorporation into the microgels.[27,28] The Cy5 donor shows a single emission peak centered at 671 nm when excited at 646 nm. When excited at 674 nm, the Cy5.5 acceptor shows an emission peak centered at 697 nm.[7] Thus, the excellent donor/acceptor overlap remains in following incorporation of the dyes into the particles, making their photophysical properties appropriate for FRET.

After observing that the spectral properties of each dye did not change when individually incorporated into core particles, equimolar quantities of both donor and acceptor dyes were randomly incorporated together into the core component of core and core/shell microgels. Figure 2 illustrates that the presence of both Cy dyes in the core does not change the VPT behavior of the microgels when monitored by PCS. The VPT temperature is approximately that of pNIPAm homopolymer microgels (∼31 °C) and is the same for both core and core/shell samples. Furthermore, there is no evidence of the VPT behavior being affected by unreacted amine groups inside the core component. A size difference is obvious between the core and core/shell particles at all temperatures, indicating that material was indeed added to the core during the shell polymerization step. Using the average particle sizes below the LCST in eq 1 yields a swollen shell thickness of ∼28 nm, while the deswollen radii ($T$ > LCST) suggest a thickness of ∼17 nm. The overall

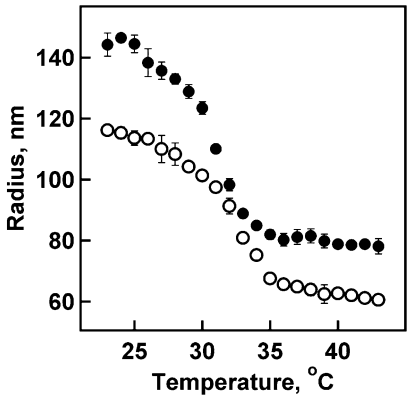


**Figure 2.** Photon correlation spectroscopy analysis of the volume phase transition behavior for Cy5/Cy5.5 labeled core microgels (open circles) and Cy5/Cy5.5 labeled core/shell microgels (solid circles). In the case of the core/shell particles, the fluorescent dyes are only bound in the core component. These measurements were made in deionized $H_2O$ and show that the covalently bound dyes have no significant effect on the particle phase transition behavior. Error bars represent one standard deviation about the average value of five measurements.

**TABLE 1: Comparison of Core and Core/Shell Particle Sizes and FRET Efficiency in the Swollen and Collapsed States**

| | radius (nm)[a] | | | intensity ratio (671:697 nm)[b] | | |
|---|---|---|---|---|---|---|
| | 23 °C | 31 °C | 43 °C | 23 °C | 31 °C | 43 °C |
| core | 116 | 97 | 61 | 1.42 | 1.15 | 0.75 |
| core/shell | 144 | 110 | 78 | 1.16 | 0.97 | 0.75 |

[a] Radii measured via photon correlation spectroscopy. [b] Wavelength intensity ratios measured via fluorescence, $\lambda_{ex} = 646$ nm.

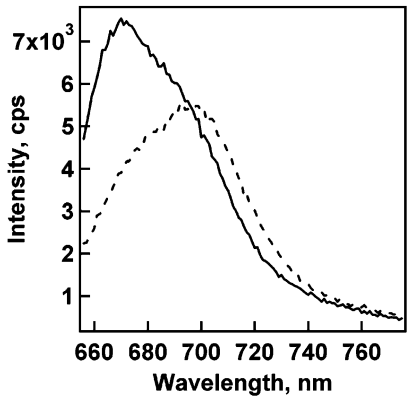


**Figure 3.** Fluorescence emission spectra of core microgels containing both Cy5 donor and Cy5.5 acceptor dyes. In the swollen state at 23 °C (solid line), there is a small amount of Cy5.5 emission, which may be due to direct Cy5.5 excitation, FRET, or a combination of the two effects. Above the phase transition temperature at 43 °C (dashed line), the average donor−acceptor distance is decreased, resulting in a decrease in the donor:acceptor intensity ratio. The sample was excited at 646 nm in both cases.

deswelling magnitude of the core/shell particle is ∼6.3-fold in volume, while the *apparent* deswelling magnitude of the shell is only ∼5.8-fold. Furthermore, the deswelling magnitude of the parent core particle is ∼6.9-fold in volume. Together, these values indicate that the core/shell particle has an overall higher network density than the parent core. From these values one can infer that the core is indeed compressed by the shell.Figure 3 shows fluorescence data for the core microgels below (23 °C) and above (43 °C) the polymer LCST. The sample was excited at 646 nm in both cases. When the microgels are in the fully swollen state at 23 °C, there is a small amount of Cy5.5

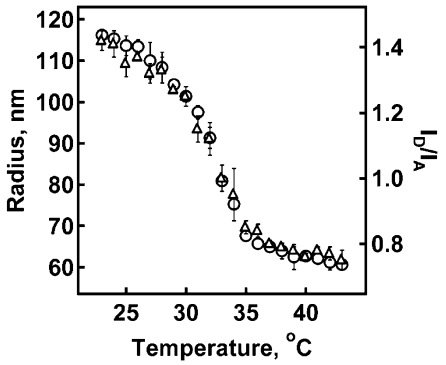


**Figure 4.** A comparison of temperature-programmed photon correlation spectroscopy analysis (circles) and fluorescence resonance energy transfer analysis (triangles) of core microgels containing both Cy5 donor and Cy5.5 acceptor molecules in deionized $H_2O$. The donor and acceptor emission intensities were monitored at 671 and 697 nm, respectively. The excitation wavelength was 646 nm. Error bars represent one standard deviation about the average value of five measurements.

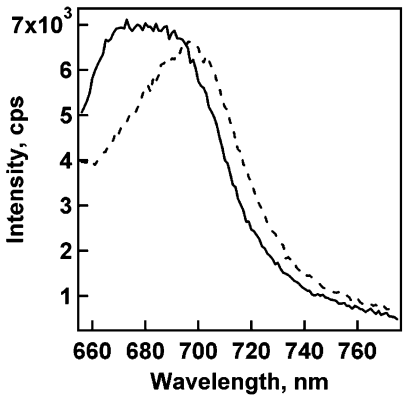


**Figure 5.** Fluorescence emission spectra of core/shell microgels containing both Cy5 donor and Cy5.5 acceptor dyes in the core component. When excited at the donor absorbance maximum of 646 nm, energy transfer and direct Cy5.5 excitation occur in the fully swollen state at 23 °C (solid line) where polymer chains in the core are hindered from swelling to their original state due to the presence of the shell. The efficiency of energy transfer increases when the core/shell particles are collapsed above the phase transition temperature at 43 °C (dashed line).

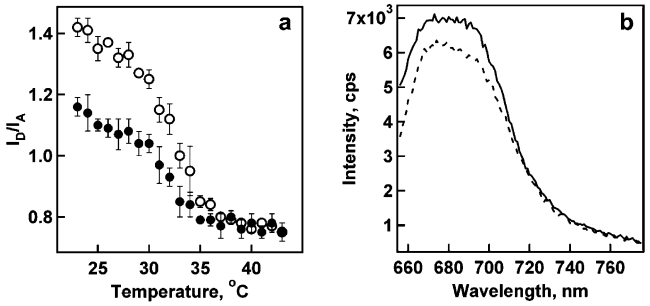


**Figure 6.** (a) Fluorescence resonance energy transfer analysis of Cy5 donor/Cy5.5 acceptor labeled core (open) and core/shell (solid) microgels in $H_2O$. When excited at 646 nm, the core/shell particles exhibit a greater degree of energy transfer than the native core below 33 °C. (b) Fluorescence analysis of core particles at 31 °C (solid line) and the core/shell particles at 23 °C. The two spectra show that approximately the same amount of energy transfer is occurring for each system at these dissimilar temperatures. Error bars represent one standard deviation about the average value of five measurements.

emission, as can be seen by comparing this curve to the emission spectrum of the singly labeled Cy5 core microgels (Figure 1). The doubly labeled microgel spectrum taken at 23 °C is somewhat broader than that of the singly labeled particles due to a small shoulder at ~697 nm, which arises from FRET between the excited-state Cy5 and the ground-state Cy5.5 moieties, as well as direct excitation of Cy5.5. However, a significant amount of energy transfer occurs as the temperature is raised to 43 °C. The fluorescence spectrum shows a broadening due to a decrease in the donor emission intensity at 671 nm and a simultaneous increase in the acceptor emission intensity at 697 nm due to FRET. In this case, the gel network collapses due to the LCST behavior of pNIPAm, which in turn decreases the average distance between the donor/acceptor pairs in the microgel. Thus, an increase in energy transfer is observed. The VPT behavior of the core microgels can be monitored with FRET by comparing the ratio of the donor and acceptor emission intensities as a function of temperature. Because of the random nature of the comonomer incorporation, the free rotation of the dyes about the tether, and the relative flexibility of the hydrogel network, we expect that the FRET signal will result from an average of all possible dye orientations. Thus, a simple ratio of the donor to acceptor emission intensities provides a good measure of the relative energy transfer efficiency in this system without the need to incorporate relative donor/acceptor orientation. As shown in Figure 4, the ratiometric FRET analysis exactly coincides with the change in particle size as a function of temperature. These data indicate that the two dyes are homogeneously incorporated throughout the microgel. If the dyes were distributed heterogeneously, one would expect to see phase transition behavior that differed from the PCS analysis.[10] Thus, the amine monomer must also be homogeneously distributed initially within the polymer matrix. Previous investigations indicate homogeneous incorporation can be expected for this particular amine monomer at the low concentrations used in this study.[29]

The spectra of core/shell microgel particles containing the donor/acceptor pair in the core are shown in Figure 5. The coupling reaction was performed after shell addition in the same manner as that for the core microgels described above. Restricted core swelling is evident from the fluorescence data in this figure. When excited at 646 nm, Cy5.5 emission is observed even when the particles are held at 23 °C, which is below the pNIPAm LCST. If we assume that the emission intensity of Cy5.5 due to direct excitation of Cy5.5 does not change following shell addition, we can attribute the increase in Cy5.5 emission to a greater degree of energy transfer in the core/shell particle relative to that in the core particle. This result suggests that the polymer network comprising the core must be less swollen as compared to its swelling prior to shell addition. In other words, the core is apparently prohibited from reswelling to its original state due to the presence of the added shell. In a manner similar to the core particles illustrated in Figure 3, the energy transfer from the core/shell particles increases when the temperature is raised above the polymer LCST. The difference in FRET between the swollen and collapsed conformations of the core/shell particles is significantly smaller than the difference observed for the core alone (Figure 3). This observation is expected, since the average donor/acceptor distance in the swollen ($T$ < LCST) core/shell particles is smaller than that in the core particles, yet the donor/acceptor distance at high temperature ($T$ > LCST) should be identical for both particles.

FRET analysis of the core and core/shell particle VPT behavior is presented in Figure 6a; the data corresponding to the core particles is the same as that presented in Figure 4. In comparison to the degree of FRET in the core, the core/shell

particles exhibit significant energy transfer at 23 °C. This behavior shows that the shell restricts the core from reswelling to its original state as shown in Figure 5 above. Furthermore, the donor:acceptor emission ratio is identical for the core and core/shell particles above the LCST, suggesting that the deswollen conformation of the core is independent of the added shell. The ratio between the donor and acceptor emission intensity at 23 °C for the core/shell particles is approximately the same as that for the core particles at 31 °C. Figure 6b shows a full spectral comparison between these two sets of data (core/shell at 23 °C and core at 31 °C). By observing the shape of the fluorescence emission spectra in this figure, it is apparent that amount of energy transfer between the donor and acceptor chromophores is approximately the same for each case, suggesting that these points represent the respective conditions where the core has the same network density. A semiquantitative value of the amount of restricted swelling can be gathered by noting that the core alone undergoes a volume decrease of 40% at 31 °C when interrogated via PCS. If the FRET data accurately report on the network density in both the native core at 31 °C and the core/shell at 23 °C, then it may be assumed that the core swelling is restricted to only 60% of its original volume in the presence of the shell. These values can now be used to determine the geometric shell thickness from eq 2, as we can now write:

$$(R_{shell})_{23C} = (R_{h,core/shell})_{23C} - (R_{h,core})_{23C} + [(R_{h,core})_{23C} - (R_{h,core})_{31C}] \quad (3)$$

where the temperatures at which the radii are measured are now indicated. This equation now indicates that the degree of core compression is equivalent to the difference in parent core radius between 23 °C and 31 °C. Inserting the correct values into eq 3, one obtains an actual geometric shell thickness of ∼47 nm as opposed to the initial PCS estimate of ∼28 nm. As stated above, the data in Figure 6a indicate that the core density (i.e. the FRET signal) is identical at $T >$ LCST for both the core and core/shell particles, we can assume that the PCS-estimated collapsed shell thickness of ∼17 nm very closely approximates the actual geometric thickness of the deswollen shell. Using this value and the new value for the swollen shell thickness of 47 nm, a new shell deswelling volume ratio of ∼8.3-fold is estimated, which is significantly larger than the initial PCS-based estimate of 5.8-fold. This new value is also larger than the deswelling ratio of the parent core of ∼6.9-fold, suggesting that the network density of the shell added in the second stage of polymerization is less that of the core formed in the first polymerization step. This is expected, since the concentration of cross-linker used in the second stage (2%) was less than that used in the core particle (5%). Thus, the combination of PCS and FRET enables the calculation of what is certainly a more realistic value for shell thickness than what is possible by PCS alone. Further studies on similar systems are underway with the aim of establishing the generality of this approach to polymer latex characterization.

## Conclusions

The structure−function relationship between the core and shell components in pNIPAm core/shell microgels has been studied via fluorescence resonance energy transfer measurements. FRET was used to observe the decreased swelling ability of the core in the presence of the added shell. Below the phase transition temperature of pNIPAm (31 °C), core particles are able to swell and achieve a volume that is limited by the polymer chain elasticity. The degree of FRET is minimal under these conditions. Core/shell particles display a significant increase of FRET due to a decreased swelling ability of the core in the presence of the added shell under the same solution conditions. Together, these studies allow for a semiquantitative determination of the actual geometric thickness of the added shell by accounting for the degree of core compression resulting from shell addition.

**Acknowledgment.** L.A.L. gratefully acknowledges financial support from the National Science Foundation, Division of Materials Research (DMR-0203707). C.D.J. acknowledges partial support from the Georgia Institute of Technology Molecular Design Institute under prime contract N00014-95-1-1116 from the Office of Naval Research, as well as a National Science Foundation Trainee Fellowship in Environmental Sciences and from the Polymer Education Research Center at the Georgia Institute of Technology.

**Supporting Information Available:** PCS data for core and core/shell particles before and after Cy-dye incorporation. This material is available free of charge via the Internet at http://pubs.acs.org.

## References and Notes

(1) Pecora, R. *Dynamic Light Scattering*; Plenum Press: New York, 1985.
(2) Jones, C. D.; Lyon, L. A. *Macromolecules* **2000**, *33*, 8301−8306.
(3) Tiarks, F.; Landfester, K.; Antonietti, M. *Langmuir* **2001**, *17*, 5775−5780.
(4) Haridas, M. M.; Bellare, J. R. *Colloids Surf., A: Physicochem. Eng. Asp.* **1998**, *133*, 165−171.
(5) Thiagarajan, V. S.; Huang, Z.; Scriven, L. E.; Schottel, J. L.; Flickinger, M. C. *J. Coll. Interface Sci.* **1999**, *215*, 244−257.
(6) Lakowicz, J. R. *Principles of Fluorescence Spectroscopy*, 2nd ed.; Kluwer Academic: New York, 1999.
(7) Schobel, U.; Egelhaaf, H. J.; Brecht, A.; Oelkrug, D.; Gauglitz, G. *Bioconjugate Chem.* **1999**, *10*, 1107−1114.
(8) Jones, C. D.; Lyon, L. A. *Macromolecules* **2003**, *36*, 1988−1993.
(9) Gan, D.; Lyon, L. A. *Macromolecules* **2002**, *35*, 9634−9639.
(10) Gan, D.; Lyon, L. A. *J. Am. Chem. Soc.* **2001**, *123*, 8203−8209.
(11) Jones, C. D.; Lyon, L. A. *Langmuir* **2003**, *19*, 4544−4547.
(12) Pelton, R. *Adv. Colloid. Interface Sci.* **2000**, *85*, 1−33.
(13) Saunders, B. R.; Crowther, H. M.; Morris, G. E.; Mears, S. J.; Cosgrove, T.; Vincent, B. *Colloid Surf., A: Physicochem. Eng. Asp.* **1999**, *149*, 57−64.
(14) Pelton, R. H.; Chibante, P. *Colloids Surf.* **1986**, *20*, 247−256.
(15) Kawaguchi, H.; Kisara, K.; Takahashi, T.; Achiha, K.; Yasui, M.; Fujimoto, K. *Macromol. Symp.* **2000**, *151*, 591−598.
(16) Tanaka, T. *Phys. Rev. Lett.* **1978**, *40*, 820−823.
(17) Heskins, M.; Guillet, J. E. *J. Macromol. Sci. Chem.* **1968**, *A2*, 1441−1455.
(18) Gan, D.; Lyon, L. A. *J. Am. Chem. Soc.* **2001**, *123*, 7511−7517.
(19) Lide, D. R., Ed. *The CRC Handbook of Chemistry and Physics*; 74th ed.; CRC Press: Boca Raton, 1994; Vol. 124.
(20) Flory, P. J. *Principles of Polymer Chemistry*; Cornell University Press: London, 1953.
(21) Fernandez-Nieves, A.; Fernandez-Barbero, A.; Vincent, B.; de las Nieves, F. J. *Macromolecules* **2000**, *33*, 2114−2118.
(22) Wu, X.; Pelton, R. H.; Hamielec, A. E.; Woods, D. R.; McPhee, W. *Colloid Polym. Sci.* **1994**, *272*, 467−477.
(23) Wu, C.; Zhou, S. *Macromolecules* **1997**, *30*, 574−576.
(24) Varga, I.; Gilanyi, T.; Meszaros, R.; Filipcsei, G.; Zrinyi, M. *J. Phys. Chem. B* **2001**, *105*, 9071−9076.
(25) Guillermo, A.; Addad, J. P. C.; Bazile, J. P.; Duracher, D.; Elaissari, A.; Pichot, C. *J. Polym. Sci., Part. B: Polym. Phys.* **2000**, *38*, 889−898.
(26) Grabarek, Z.; Gergely, J. *Anal. Biochem.* **1990**, *185*, 131−135.
(27) Mujumdar, R. B.; Ernst, L. A.; Mujumdar, S. R.; Lewis, C. J.; Waggoner, A. S. *Bioconjugate Chem.* **1993**, *4*, 105−111.
(28) Mujumdar, S. R.; Mujumdar, R. B.; Grant, C. M.; Waggoner, A. S. *Bioconjugate Chem.* **1996**, *7*, 356−362.
(29) Meunier, F.; Elaissari, A.; Pichot, C. *Polym. Adv. Technol.* **1995**, *6*, 489−496.